Green and Sustainable Environments

Green and Sustainable Environments **1** (2026) 10
https://doi.org/10.62755/gsenv.2026.10
journal homepage: pubs.greensus.org/gsenv

Check for updates



RESEARCH PAPERS

PET Accelerates the Decomposition of HDPE During Co-Pyrolysis: A Non-Additive Interaction from Thermogravimetry to Bench Scale

Aulia Annas Mufti[1], Neza Rahayu Palapa[2], Muhamad F. Arif[3], Tarmizi Taher[1,4,*]

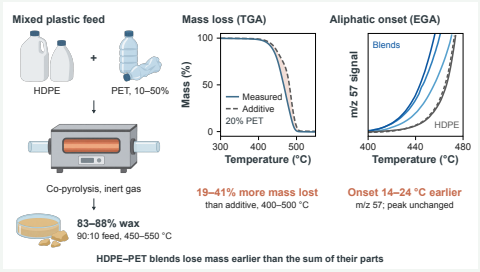
[1] *Department of Environmental Engineering, Institut Teknologi Sumatera, South Lampung 35365, Indonesia*
[2] *Department of Chemistry, Faculty of Mathematics and Natural Sciences, Universitas Sriwijaya, Indralaya, Ogan Ilir 30662, Indonesia*
[3] *Materials Engineering, Institut Teknologi Sumatera, South Lampung 35365, Indonesia*
[4] *Center for Green and Sustainable Materials, Institut Teknologi Sumatera, South Lampung 35365, Indonesia*

* **Corresponding author**: tarmizi.taher@tl.itera.ac.id

ARTICLE HISTORY: Received: September 13, 2026 · Revised: November 18, 2026 · Accepted: November 18, 2026

ABSTRACT

Post-consumer polyolefin waste sent to pyrolysis commonly carries poly(ethylene terephthalate) (PET), yet yield and kinetic models for such feeds often treat their components as decomposing independently. We tested that assumption by comparing the thermogravimetric response of blends of high-density polyethylene (HDPE) and PET with the mass-weighted sum of the pure polymers measured in the same campaign, in single runs at 10, 20 and 50 % PET. All blends lost mass faster than the additive prediction, by 19–41 % of the initial mass between 400 °C and 500 °C, and the sign of the deviation held in two campaigns run a month apart at 9.8 °C min^{-1} and 20.3 °C min^{-1}, although the ranking of the blends did not. Evolved-gas analysis placed the volatile maximum of every blend within 5 °C of HDPE, but the aliphatic channel (m/z 57) of the blends left the baseline 14–24 °C below that of HDPE, against a repeatability of 2 °C. Micro-pyrolysis at 600 °C gave aromatics and acids at 0.9–11.4 % of the identified product area for blends with 10 to 50 % PET, against 50.4 % for PET alone. In a horizontal tube reactor, a 90:10 HDPE:PET feed held for 60 min at 450–550 °C gave 83–88 % wax and at most 5.1 % GC-quantifiable liquid, with mass balances closing to 92–95 %. Without a pure-HDPE reactor run, this slate cannot be assigned to PET. The additive superposition of pure-polymer curves therefore underestimates how early a PET-bearing polyolefin feed loses mass, and the evolved-gas profiles show that this earlier loss includes an earlier onset of the polyolefin fraction.



KEYWORDS *co-pyrolysis; mixed plastic waste; HDPE; PET; polymer interaction; thermogravimetry*

1. INTRODUCTION

Of the roughly 6300 million tonnes of plastic waste generated worldwide by 2015, about 9 % had been recycled and 79 % had accumulated in landfills or the natural environment [1]. How much escapes collection depends largely on population and on the quality of waste management [2], and scenario modelling finds that 710 million tonnes enter aquatic and terrestrial ecosystems between 2016 and 2040 even under immediate, concerted action on consumption, collection and recycling [3]. Mechanical recycling, which reprocesses the polymer by melting, depends on a clean and uniform feed that post-consumer waste seldom supplies [4]. A single packaging waste stream can contain up to nine polymers together with metals and halogens at 1 to 3000 ppm, impurities that in many cases prevent closed-loop recycling [5]. Material flow analysis put the end-of-life recycling rate of post-consumer plastic packaging in the EU27 at 14 % in 2017, with significant losses of target polymers at both the sorting and the recycling stage [6].

Pyrolysis does not require that purity. It converts mixed plastic waste into oil, wax and gas [7, 8], and its robustness and feed flexibility have made it, with gasification, a leading route for chemical recycling [9]. Feed flexibility does not make the feed irrelevant, however, and PET is a recurring blending partner: sorted post-consumer packaging streams destined for pyrolysis still contain it, and enriching them in polyolefins at pilot scale meant removing mostly PET [10, 11]. The oxygen that PET carries is a liability downstream. Post-consumer pyrolysis oils contain about 1250 ppm oxygen against a steam-cracker feed limit of 100 ppm, and contaminants of this kind drive corrosion, fouling and catalyst poisoning [12]. PET also yields solids. Terephthalic acid appeared in the wax from a mixed feed carrying 15 % PET by mass [13], and PET processed alone in a mobile pyrolysis plant gave mostly solid product that blocked the pipework [14]. Removing PET is not a complete answer either. Polyolefin enrichment by sorting improved the oil only to a limited extent, because oxygen- and chlorine-bearing species remained [11], while recovering PET as terephthalic acid before pyrolysis raised the yield and quality of the liquid at the cost of an added depolymerisation step [15]. For most pyrolysis units, the practical question is how a polyolefin feed behaves with some PET still in it.

The two polymers decompose by different chemistry. High-density polyethylene (HDPE) degrades by scission of its saturated hydrocarbon backbone [16], in a single sharp mass-loss step with negligible residue [17]. Poly(ethylene terephthalate) (PET) decomposes through ester scission, releasing acetaldehyde, CO and CO_2 [18] as well as terephthalic acid [13], and leaves a carbonaceous residue that reached about 20 % of the initial mass for waste PET under nitrogen [19]. Kinetic parameters for each polymer alone are well established [20, 21]. Their decomposition windows, however, overlap. At 15 °C min^{-1}, PET degrades over 394–471 °C and HDPE over 449–497 °C, and a blend of the two spans 417–495 °C with an onset between them [17]. In a blend, PET therefore releases its oxygenated volatiles into polyethylene that has not yet begun to decompose on its own, which is the condition under which one polymer could alter the degradation of the other.

Whether it does is where the evidence divides. Mixed-plastic yield and kinetic models commonly superpose pure-component behaviour weighted by composition, and for some mixtures the approximation holds. A superposition model reproduced the oil and wax yield of sorted packaging-waste mixtures to within 8 percentage points [10], and superposed pure-polymer kinetics predicted the thermogravimetric degradation of heteroatom-free polymer blends accurately [22]. The same stud-

e-ISSN 3124-4610 · © 2026 The Authors · CC BY 4.0 OPEN ACCESS

ies located where superposition fails. Above 33 % PET by mass, mixed streams gave more solid than predicted and an aromatic carbon yield that could not be predicted at all, which the authors attributed to PET interacting with the other polymers [10]. Blends containing oxygen-, nitrogen- or chlorine-bearing polymers showed accelerated reactions and coke formation that the superposed kinetics did not capture [22], and mixtures representative of polyolefin and polyester waste showed strongly conversion-dependent activation energies that the authors attributed to interactions lowering them [23]. Comparing measured heat release rates with mass-weighted sums, Snegirev et al. [24] found HDPE–PET among the most strongly interacting of the binary mixtures they examined. Interaction is not confined to heteroatom-bearing pairs, and it acts in both directions: HDPE–PP mixtures rich in PP began to degrade below either pure polymer [25], whereas mixtures of polyolefins with polystyrene co-pyrolysed later than the pure polymers [26]. At reactor scale, mixing polystyrene 1:1 with each of the other major plastics gave more gas and less oil and wax than the individual plastics predicted [27].

Three limitations keep this evidence from settling the case of a polyolefin feed that carries a modest amount of PET. First, where PET-bearing blends have been tested against superposition, the result is reported for heteroatom-containing polymers as a class [22] or for streams above 33 % PET [10]. Among these studies, evidence specific to HDPE–PET comes from heat release rather than mass loss [24], or from apparent kinetic parameters fitted to a single blend [17], which reproduce that blend's curve but do not by themselves show how far it departs from its components. Second, a deviation of a few per cent of the initial mass is small enough to arise from the temperature programme, or from reference curves recorded in a different session. Kinetic parameters evaluated from a single heating rate are known to be unreliable [28], and the degree of mixing is itself a variable in such tests [22]. Separating an interaction from an artefact therefore requires pure-component references measured in the same campaign as the blends, and a repeat of the whole test under an independent temperature programme. Third, milligram-scale evidence does not transfer automatically to a reactor. Heat and mass transfer, heating rate and residence time differ between the scales and strongly affect how plastics degrade [9], and analytical pyrolysis of polymer mixtures can itself generate cross-products that neither polymer gives alone [29]. Connecting an interaction to process design means following it from mass loss through evolved gases and products to a mass-closed reactor experiment on the same feed. What is missing, therefore, is a direct additivity test for HDPE–PET at the PET loadings of a contaminated polyolefin stream, made against same-campaign references, repeated under a second temperature programme, and followed from thermogravimetry to a reactor.

Herein we test additivity directly for HDPE–PET blends containing 10, 20 and 50 % PET and follow the consequences from milligram to gram scale. The measured thermogravimetric response of each blend is compared with the mass-weighted sum of pure-polymer curves from the same campaign, in two campaigns run a month apart under different temperature programmes, at 9.8 °C min^{-1} and 20.3 °C min^{-1}. Evolved-gas analysis and pyrolysis–gas chromatography/mass spectrometry then locate the deviation in temperature and in product class, and bench-scale experiments in a horizontal tube reactor at 450–550 °C close the mass balance on a 90:10 HDPE:PET feed. Every blend lost mass faster than additivity predicts, by up to 41 % of the initial mass between 400 °C and 500 °C, and the sign of the deviation held in both campaigns. Apart from two repeated evolved-gas acquisitions, each measurement is a single run, and the conclusions are drawn at that level. No catalyst is used anywhere in this work: the aim is the thermal behaviour of the mixture itself, which is the baseline any catalytic scheme for PET-bearing polyolefin waste has to be measured against.

2. EXPERIMENTAL

2.1 Materials

HDPE and PET were both obtained from Shinko Plastics Co., Ltd. (Japan). HDPE was a fine powder and used as received; PET pellets were crushed and sieved below 150 µm before use. Samples contained 0, 10, 20, 50 and 100 % PET by mass. Blends were not drawn from a bulk mixture: for every run, the two powders were weighed separately for that charge and mixed by stirring until homogeneous, so that each charge carried its nominal composition. The one exception is the 90:10 mixture of the Oct 2020 series, used for evolved gas analysis and analytical pyrolysis, which was taken from a 1 g mixture of 0.100 g PET and 0.901 g HDPE. Weighing each charge fixes its composition. How intimately the two powders were in contact within a charge of a few milligrams was not characterised. No catalyst or additive was used in any experiment reported here.

2.2 Thermogravimetric Analysis

Thermogravimetric analysis (TGA) was carried out on a Thermo plus EVO2 TG-DTA (Rigaku Corp., Japan), with 4.9–11.3 mg of sample in an alumina pan (Table 1). Each composition was run once under each programme. Every run opened with a 5 min conditioning hold at 28 °C under N_2 at 100 mL min^{-1}; the pyrolysis stage that follows ran under N_2 at 50 mL min^{-1} and the oxidation stage under air at the same flow. Two programmes were used. The first was a straight ramp under N_2 from ambient to 800 °C at a set 20 °C min^{-1} (measured 20.3 °C min^{-1}), which gives the decomposition profile against temperature; the air stage to 850 °C that follows lies outside the analysed window. The second was a three-stage programme: a ramp under N_2 to a set 550 °C at a measured 9.8 °C min^{-1}, an isothermal hold for 120 min at a measured 560 °C, and a switch to air for 30 min at 600 °C, ending at 610 °C. This final stage oxidises whatever residue survived pyrolysis, separating volatile release from the solid left behind.

Heating rates are those measured from the recorded temperature–time trace over 150–500 °C, not the nominal set points. Plateau temperatures measured at the sample sat 10–27 °C above set point, the offset widening with ramp rate. Throughout this paper, TGA temperatures are measured sample temperatures unless a value is named as a set point; temperatures in evolved gas analysis–mass spectrometry (EGA-MS) are programme temperatures calculated from the acquisition time; and reactor temperatures are set points.

Isothermal runs on the 50 % PET blend were held for 120 min at set points of 450, 500 and 550 °C under N_2, reached at 20 °C min^{-1}.

Derivative thermogravimetric (DTG) curves were obtained by Savitzky–Golay smoothing of the TG signal (third-order polynomial, 51-point window) followed by numerical differentiation with respect to temperature. Onset temperatures are the point at which the smoothed TG falls below 98 % of the 100–250 °C baseline.

2.3 Additivity Test

For each blend of PET mass fraction x, the measured TG curve was compared with the mass-weighted sum of the pure-component curves from the same campaign (Eq. (1)). All curves were resampled onto a common 300–550 °C grid at 0.5 °C spacing before subtraction, so that the deviation is read at matched temperatures rather than matched times. The test was applied independently to each campaign, using the pure HDPE and pure PET runs measured in that campaign under the same programme as the blends. Because blend and references are compared at the same measured temperature within one programme, the offset between set point and measured temperature does not enter the deviation.

2.4 Evolved Gas Analysis–Mass Spectrometry

EGA-MS was run on a multi-shot micro-pyrolyser (EGA/PY-3030D; Frontier Laboratories Ltd., Japan) mounted directly on a GC-MS (GCMS-QP2020; Shimadzu Corp., Japan), under helium. Evolved gases were split 1/200 and carried to the detector through a deactivated metal transfer tube (UA-DTM-2.5N, 2.5 m × 0.15 mm i.d.; Frontier Laboratories) without chromatographic separation; the GC oven, pyrolyser interface and MS interface were all held at 300 °C. The temperature programme ramped from 100 °C to 600 °C at 20 °C min^{-1} after a 1 min hold, and retention time was converted to sample temperature on that basis. Acquisition ran from 1.00 to 26.00 min at a 300 ms scan event. Extracted-ion profiles were taken at m/z 41, 44, 55, 57, 65, 69, 71, 77, 91, 97, 105, 111, 121 and 149. For one of the HDPE acquisitions and for the 90:10 mixture a shorter set was extracted, m/z 43, 57, 71, 97 and 111, with 149 added for the mixture. HDPE and the 90:10 mixture were each acquired twice, in the Oct 2020 series. PET and the 10, 20 and 50 % PET blends were acquired once. Sample masses were 1.0–1.1 mg, except for one HDPE acquisition at 0.5 mg (Table 2). The charges of the blend series

© 2026 The Authors | CC-BY 4.0

Table 1. Sample mass of each TGA run, in mg. Each entry is one run. The isothermal runs on the 50 % PET blend used 6.1 mg, 5.6 mg and 5.9 mg at set points of 450, 500 and 550 °C.

Composition	Straight ramp, 20.3 °C min^{-1}	Three-stage, 9.8 °C min^{-1}
HDPE	6.9	6.0
10 % PET	4.9	5.4
20 % PET	5.5	6.4
50 % PET	6.5	6.8
PET	6.1	11.3

were weighed as 0.1 mg PET with 0.9 mg HDPE, 0.24 mg with 0.82 mg, and 0.55 mg with 0.58 mg, so that the blends named 20 and 50 % PET contained 23 % and 49 % PET in EGA-MS.

The onset of an extracted-ion profile was read after subtracting its baseline (the median over 250–320 °C) and smoothing with a 2 °C moving average, as the temperature at which the rising edge first reached 5, 10 and 50 % of the profile's own maximum. Because each profile is normalised to itself, these temperatures do not depend on the absolute response of the detector.

2.5 Pyrolysis–Gas Chromatography/Mass Spectrometry

Pyrolysis–gas chromatography/mass spectrometry (Py-GCMS) used the same pyrolyser and GC-MS, with one run per composition. Samples were weighed into a deactivated stainless-steel cup plugged with quartz wool. Pyrolysis was at 600 °C; evolved volatiles were cryo-trapped at the GC inlet and separated on a metal capillary column (Ultra ALLOY UA + -5, 5 % diphenyl / 95 % polydimethylsiloxane, 30 m × 0.25 mm i.d., 0.25 µm film; Frontier Laboratories). Peaks were identified against the F-Search (Frontier Laboratories) and NIST mass spectral libraries.

Peaks were grouped into compound classes by keyword matching against the library hit name. Hits naming an element that neither polymer can supply (F, Cl, Br, I, N, P, S or Si) were treated as misassignments and excluded; the largest such family is a set of long-chain fluorinated esters that the library returns for the long-chain aliphatic spectra a cracking polyolefin gives. The classes are a coarse grouping over the identifications that survive that check, expressed as fractions of total ion current (TIC) area, and are not a quantitative speciation.

2.6 Bench-Scale Pyrolysis

Pyrolysis was carried out in a custom horizontal quartz tube reactor of 7.5 mm inner diameter, heated by an electric furnace. A charge of about 2 g (1.896–2.002 g for the 90:10 runs) was placed at the centre of the tube and the reactor purged with argon for 30 min, heated at 20 °C min^{-1} to the target temperature, and held there under a continuous 20 mL min^{-1} argon flow (60 min for the 90:10 feed, 120 min for the 80:20 feed). Condensable products were collected in two impingers in series, the first holding 50 mL of adamantane-in-acetone internal standard solution in an ice bath and the second in a −30 °C bath (PSL-1400; Eyela); gas leaving the second impinger was collected in an aluminium gas bag. Wax condensed at the downstream end of the tube, outside the furnace. Wax and solid residue were determined by weighing before and after each run: the wax as the mass gained by the tube, and the residue as the mass gained by the vessel that held the charge. Runs were made on a 90:10 HDPE:PET feed at 450, 500 and 550 °C, and on an 80:20 feed at 550 °C, once at each condition. The schematic is shown in Fig. 1.

2.6.1 Product analysis

Liquid products were quantified on a Shimadzu GC-2010 Plus with autosampler and flame ionisation detection, on a DB-5 capillary column (Agilent J&W); the oven was held at 40 °C for 3 min, ramped at 15 °C min^{-1} to 250 °C and held for 8 min. They were identified on a GC-MS (GCMS-QP2020; Shimadzu) with a DB-5 column (Agilent J&W) under the same oven programme. Both were referenced to an adamantane internal standard, added as a 2.505 mg g^{-1} solution to give 97–100 mg per sample. Response factors were taken from four-point calibrations: 0.739 for aliphatics, the mean of the through-origin slopes for heptane, methylcyclohexane and octane, and 0.9417 for benzene, toluene and xylenes (BTX). Peaks were assigned to BTX, C_6–C_{12} and $C_{12}{}^+$ by retention time against those standards, with the solvent front below 2.45 min excluded; the liquid yield reported in Table 4 is the sum of those three classes, not a weighed fraction. Permanent gases were quantified on a gas chromatograph (7890B; Agilent Technologies) fitted with molecular sieve 5A and HayeSep Q columns and dual thermal conductivity detection, against an argon internal standard and referenced to an equal-volume calibration mixture, and converted to mass at STP. Ethane had no response factor of its own and was quantified on that of methane; ethylene, C_3–C_4 hydrocarbons and CO were not calibrated.

3. RESULTS AND DISCUSSION

3.1 Thermal Decomposition of HDPE–PET Blends

Two thermogravimetric programmes were used. A straight ramp at 20.3 °C min^{-1} under N_2 gives the decomposition profile as a function of temperature. A three-stage programme (a ramp at 9.8 °C min^{-1} to 560 °C under N_2, an isothermal hold, then air at 600 °C) separates volatile release from the residue left to burn off. The two campaigns ran a month apart, each with its own pure-component references.

3.1.1 Pure components and composition trends

Pure HDPE decomposed in a single sharp step with an onset of 425 °C and a DTG maximum at 485 °C, and left no measurable residue, the profile reported for HDPE elsewhere [17]. Pure PET began to lose mass 26 °C earlier, at 399 °C, peaked at 448 °C, and left 13 % char at 550 °C. The second programme gave a similar value, 15.7 % at the end of its ramp and 13.8 % after a 120 min hold at 560 °C (Section 3.1.3), so a char yield of 13–16 % is reproducible for this PET. It is lower than the about 20 % reported for waste PET under nitrogen [19] and the up to 24 % reported for slow pyrolysis [30]. PET char depends on the material and on how it is pyrolysed. The sample here was a ground pellet below 150 µm, pyrolysed as a few milligrams in flowing N_2, conditions under which volatiles leave the solid quickly. The measurements do not show which of these differences accounts for the lower yield.

Blends fell between the two and moved monotonically with PET content. The onset decreased from 425 °C for HDPE through 410 °C (10 % PET) and 406 °C (20 % PET) to 403 °C (50 % PET), and the DTG maximum fell from 485 °C to 455 °C over the same range while the peak broadened. Char at 550 °C rose with the PET fraction: nil for HDPE and the 10 and 20 % PET blends, 4 % at 50 % PET and 13 % for PET alone, placing the char origin in the PET fraction (Fig. 2).

3.1.2 Blends decompose faster than additivity predicts

Composition trends of this kind are usually read as interpolation between the two polymers, and mixed-plastic yield and kinetic models are commonly built on exactly that assumption [10, 22]. If the polymers decomposed independently, a blend with PET mass fraction x would follow

$$\mathrm{TG}_{\mathrm{additive}}(T) = (1-x)\,\mathrm{TG}_{\mathrm{HDPE}}(T) + x\,\mathrm{TG}_{\mathrm{PET}}(T), \tag{1}$$

and the difference between the measured curve and Eq. (1) is taken here as the measure of interaction.

Every blend decomposed faster than Eq. (1) predicts. In the campaign at 20.3 °C min^{-1} the measured mass fell below the additive prediction by 19.2 % of the initial mass at 480 °C (10 % PET), 29.4 % at 477 °C (20 % PET) and 24.4 % at 476 °C (50 % PET), with the deviation exceeding 5 % across roughly 440–500 °C. The campaign at 9.8 °C min^{-1} reproduced the sign and the scale of the effect, with maxima of 40.9 %, 25.6 % and 26.9 % for the same three blends, but not their ordering. The window lay lower, at 400–485 °C, in the campaign with the lower heating rate (Fig. 3). The two programmes differ in more than heating rate, so this comparison shows that the effect is not specific to one programme. It is not a measurement of how the effect depends on heating rate.

© 2026 The Authors | CC-BY 4.0

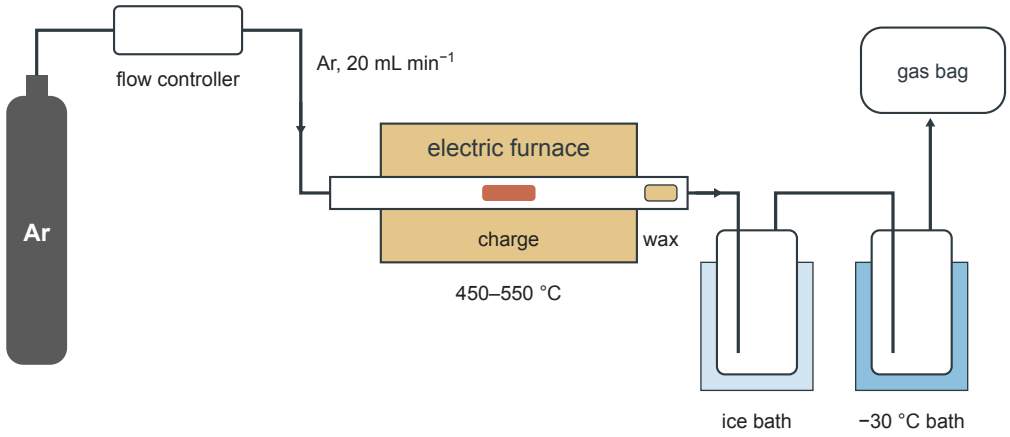


Figure 1. Bench-scale horizontal quartz tube reactor. Wax condenses on the tube end outside the electric furnace; arrows give the direction of argon flow.

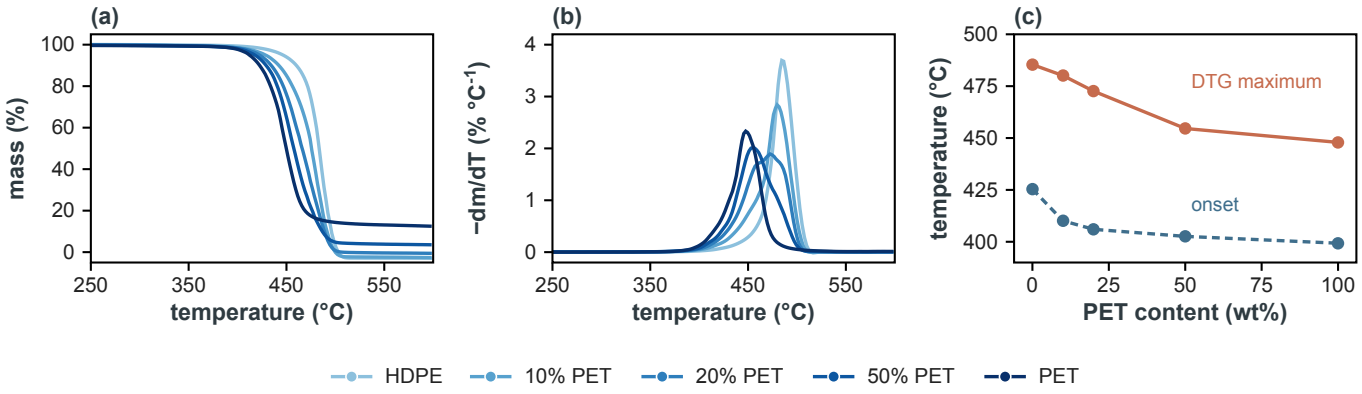


Figure 2. Non-isothermal TGA of HDPE–PET blends at 20.3 °C min^{-1} under N_2. (a) mass loss; (b) rate of mass loss, plotted as $-dm/dT$; (c) onset temperature and DTG maximum against PET content. Colour encodes PET content throughout.

Each composition was run once per programme, so these deviations carry no run-to-run standard deviation. The second campaign is the available check on their reproducibility. For a given blend, the maxima of the two campaigns differ by 2.5–21.7 % of the initial mass, a spread that includes the change of programme, while the smallest of the six maxima is 19.2 %. The sign and the order of magnitude of the deviation are therefore reproduced, and the ranking of the blends is not.

Expressed as temperature, every blend reached half of its initial mass 6.5–16.5 °C earlier than Eq. (1) predicts. Heat-transfer limitations can distort milligram-scale TGA when the sample mass is too large [31], and sample masses were not matched in every case (Table 1): the PET reference of the 9.8 °C min^{-1} campaign weighed 11.3 mg against 5.4–6.8 mg for the blends. A heavier reference lags in temperature, which moves the additive prediction to higher temperature in proportion to the PET fraction and would enlarge the apparent deviation most at 50 % PET. In the 20.3 °C min^{-1} campaign all masses lay within 4.9–6.9 mg. The closest match is the 50 % PET blend, which weighed 6.5 mg, between its HDPE (6.9 mg) and PET (6.1 mg) references, and still reached half mass 13.5 °C early. The 10 and 20 % PET blends were 1.4–2.0 mg lighter than their HDPE reference, and a contribution of thermal lag to their deviations cannot be excluded.

The ranking of the blends differed between the campaigns: 20 % PET showed the largest deviation at 20.3 °C min^{-1} and 10 % PET at 9.8 °C min^{-1}. With one run per composition and campaign, these data do not resolve how the deviation depends on PET content. They show only that in neither campaign did it increase in proportion to the PET fraction, and a composition dependence that changes with the proportions has been reported for PET–polyethylene film blends [32]. The direction of the deviation agrees with TG-FTIR of PET–HDPE mixtures, in which HDPE degraded at a lower temperature than on its own [33].

PET decomposes in the window where the deviation opens. Its ester linkages are proposed to break through a six-membered cyclic transition state into vinyl- and carboxyl-terminated fragments [34], and the evolved-gas measurements of Section 3.2 place the PET-derived evolution ahead of the polyolefin event. Two kinds of contribution could produce the deviation, and the present experiments do not separate them. Chemically, these fragments, or radicals and acids formed from them, may initiate scission of polyethylene chains that have not yet begun to break on their own, and interactions in mixed plastics have been reported to depend mainly on the reactivity of the intermediate degradation products [32]. Physically, PET decomposing inside a shared melt may change how heat reaches the polyethylene and how its volatiles leave. Neither route is demonstrated here. Showing transfer between the two polymers would need isotopic labelling or trapping of the intermediate.

3.1.3 Stage-resolved mass loss

The three-stage programme separates what leaves as volatiles from what remains to be burned. For HDPE and the 10 % and 20 % PET blends, essentially all mass was lost during the ramp; the isothermal hold at 560 °C removed a further 0.02–0.71 % and the air stage less than 0.05 %. The 50 % PET blend retained 4.1 % into the isothermal hold and lost all of it there, leaving 0.02 % for the air stage, whereas PET alone still held 13.8 % after the hold and lost 12.9 % in the air stage. Volatile release is therefore complete by the end of the ramp for HDPE-rich blends.

The residue does not follow the mass-weighted sum at 50 % PET: that sum predicts about 6.4 % burning off in the air stage, against 0.02 % mea-

© 2026 The Authors | CC-BY 4.0

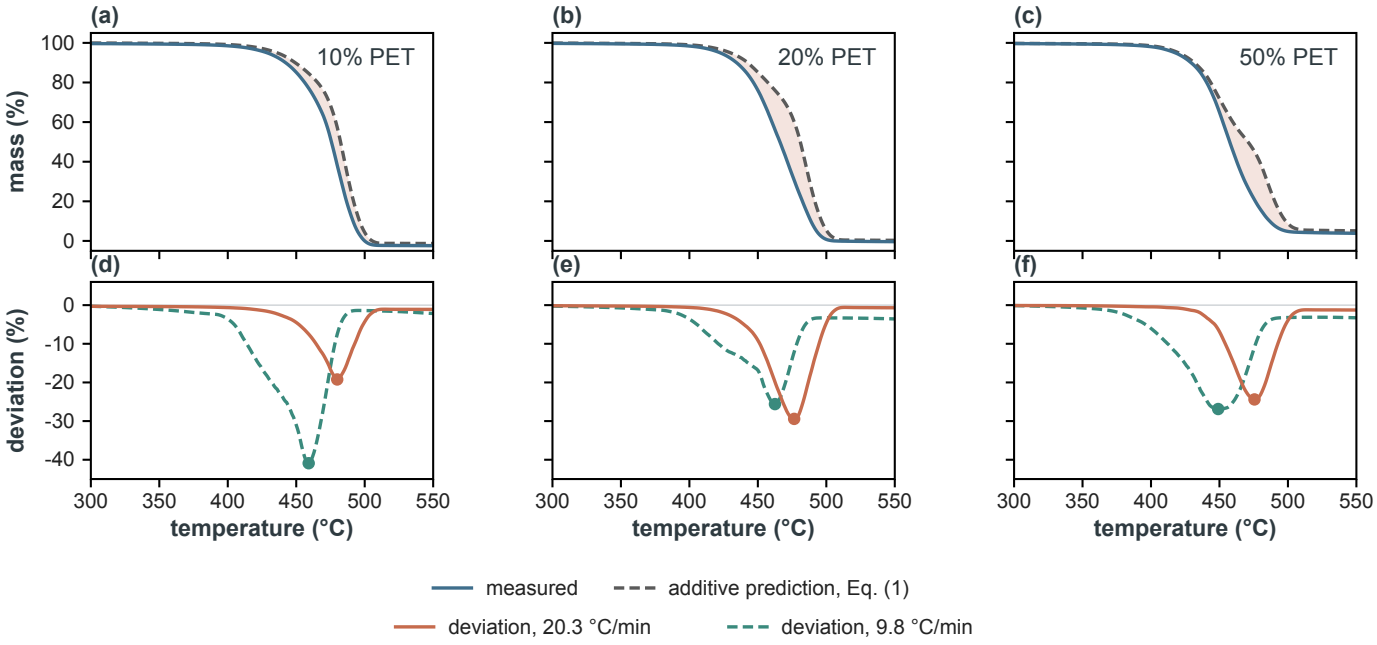


Figure 3. Measured decomposition against the additive prediction of Eq. (1). (a–c) TG at 20.3 °C min^{-1} for each blend (solid) with the mass-weighted sum of the pure components (dashed); the shaded area is the difference. (d–f) that difference for both campaigns, at 20.3 and 9.8 °C min^{-1}; filled circles mark the maximum deviation. Each campaign's prediction uses the pure components measured in that same campaign.

sured, and the straight ramp gives the same shortfall at 550 °C, 3.8 % against a predicted 5.1 %. The shortfall contrasts with microscale combustion calorimetry of binary HDPE mixtures, HDPE–PET among them, in which char yield varied almost linearly with composition [24]. It also runs opposite to mixed packaging streams above 33 % PET, which gave more solid than superposition predicted [10], and to the coke formation reported for blends of heteroatom-bearing polymers [22]. The cause was not investigated. Hydrogen transfer from the decomposing polyethylene to PET-derived fragments, capping them before they condense into carbonaceous residue, is one possible route, and a physical effect of the molten polyolefin on how PET volatiles escape is another.

Holding the 50 % PET blend at temperature adds almost nothing to this. Reaching set points of 450, 500 and 550 °C at 20 °C min^{-1} left 5.9–8.7 % of the initial mass when the hold opened, and 120 min at temperature removed a further 1.1–1.9 % against the 91–94 % already lost on the ramp. Devolatilisation is complete below 480 °C, the measured plateau of the lowest set point, and what survives is the residue the air stage burns off. The bench-scale reactor gives the same answer on a charge some 300 times larger: at 450 °C, 93.1 % of a 90:10 feed left as wax, liquid and gas (Table 4).

3.2 Evolved Gas Analysis

EGA-MS tracks when volatiles leave the sample. Pure HDPE gave a single intense peak at 498 °C, 13 °C above its DTG maximum on a similar ramp. Pure PET gave a much weaker response peaking at 456 °C, roughly an order of magnitude below HDPE, consistent with its lower volatile yield and higher char yield [19]. The same ordering, PET before HDPE, appears in EGA of the pure polymers at 10 °C min^{-1}, where PET peaked at 410 °C and HDPE at 474 °C [35].

All blends peaked between 494 °C and 498 °C, within 5 °C of HDPE and not at the composition-weighted position between the two pure components (Fig. 4). Adding PET broadened the profile and lowered its intensity, and the 50 % PET blend resolved a second feature at 463 °C reaching 0.72 of its maximum, but the position of the maximum stayed with the polyolefin.

Splitting that blend by channel identifies the earlier feature, using ions that EGA of the pure polymers assigns to PET (*m/z* 149) and to polyethylene oligomers (*m/z* 57) [35]. The terephthalate fragment at *m/z* 149, at background in HDPE, peaked at 454 °C; the aliphatic fragment at *m/z* 57, at background in PET, peaked at 496 °C. The two events are 43 °C apart in one sample, and *m/z* 149 peaked between 451 °C and 457 °C in every PET-bearing sample, so the PET fraction released its volatiles ahead of the polyolefin at each loading tested.

The deviation of Section 3.1.2 therefore does not appear as a shift of the main evolution peak. It falls in the 440–500 °C window between the two events, where the TIC is dominated by the rising polyolefin edge, and that edge is where the blends differ from HDPE.

TGA records the mass of the whole sample and cannot say which polymer loses it earlier. The aliphatic channel can. The *m/z* 57 profile of every blend reached its maximum at 494–498 °C, as HDPE did (495 °C and 498 °C), but left the baseline at a lower temperature (Fig. 5, Table 2). HDPE reached 5 % of its maximum at 451 °C and 452 °C in its two acquisitions. The blends reached it at 436–438 °C (10 % PET, three acquisitions), 429 °C (20 %) and 428 °C (50 %), which is 14–24 °C below the mean of the two HDPE acquisitions. At this level and at 10 % of the maximum, repeat acquisitions of one composition agreed within about 2 °C. The shift became smaller further up the rising edge, falling to 10 °C or less at half maximum, where the repeats also agreed less closely (6 °C), and it vanished at the maximum. Unlike the TGA deviation, it followed PET content, increasing from 10 to 20 % PET and levelling off between 20 and 50 %.

PET itself contributes little to this channel. In pure PET, *m/z* 57 amounted to 0.019 of *m/z* 149, and subtracting that proportion of each blend's *m/z* 149 profile removed at most 4.6 % of its *m/z* 57 signal over 420–470 °C and moved the onset by less than 2 °C. The other aliphatic fragments recorded (*m/z* 55, 69, 71, 97 and 111) shifted by similar amounts. The earlier mass loss of the blends therefore includes an earlier release of aliphatic fragments, which only the polyethylene supplies in quantity. Sample mass does not account for the shift. The blend charges weighed 1.0–1.1 mg, as did one of the HDPE references, and the two HDPE acquisitions, at 0.5 mg and 1.1 mg, gave onsets within 1 °C of each other. This result is limited in three ways. First, *m/z* 57 is a marker for the polyolefin and not a measure of its mass. Second, the 20 and 50 % PET blends were each acquired once. Third, the HDPE references belong to the earlier series, so that only the 90:10 mixture was acquired in the same series as its reference.

The two techniques constrain the interaction differently. TGA gives the mass lost and cannot assign it to either polymer. EGA-MS assigns the evolved species by fragment but, being uncalibrated, gives no mass. Both

© 2026 The Authors | CC-BY 4.0

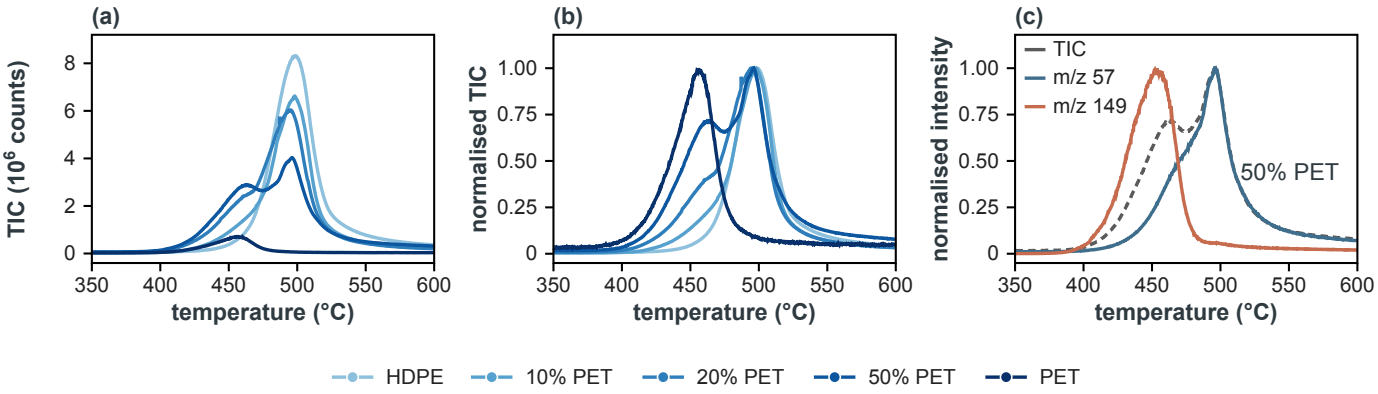


Figure 4. EGA-MS under the same ramp. (a) total ion current; (b) TIC normalised to each sample's own maximum; (c) the 50 % PET blend by channel, each normalised to its own maximum, where m/z 57 is the aliphatic fragment and m/z 149 the terephthalate fragment.

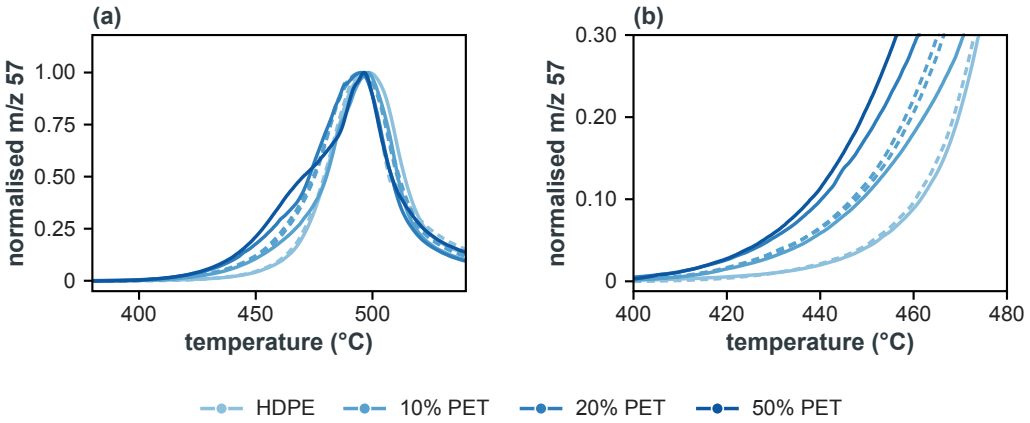


Figure 5. Onset of the aliphatic channel. (a) m/z 57 profiles normalised to their own maxima; (b) the rising edge. Solid lines are HDPE and the 10, 20 and 50 % PET blends; dashed lines are the second HDPE acquisition and the two acquisitions of the 90:10 mixture.

Table 2. Temperature (°C) at which the m/z 57 profile first reached 5, 10 and 50 % of its own maximum, and temperature of the maximum. Each row is one acquisition; mass is the sample mass in mg.

Sample	Series	Mass	5 %	10 %	50 %	Maximum
HDPE	Oct 2020	0.52	451.3	460.4	479.3	495.0
HDPE	Oct 2020	1.06	452.4	461.6	479.8	497.5
90:10 HDPE:PET	Oct 2020	1.07	435.8	447.7	475.2	495.8
90:10 HDPE:PET	Oct 2020	1.04	435.8	446.8	474.6	494.5
10 % PET	Mar 2021	1.0	437.6	448.9	480.3	498.3
20 % PET	Mar 2021	1.06	429.2	440.2	472.9	495.0
50 % PET	Mar 2021	1.13	427.8	438.0	470.3	496.3

follow the rate of volatile release under a temperature ramp, so what they establish is kinetic: mass leaves earlier in the blend. Neither measures a heat of reaction or an equilibrium composition, and the data place no constraint on the thermodynamics of the decomposition.

3.3 Product Identification

Micro-pyrolysis at 600 °C resolved between 193 and 353 peaks per sample. A large share of the peak area carries a library name that neither polymer can account for, from 32 % for PET rising to 56 % for the 10 % PET blend (Table 3). The fractions below are therefore taken over the identifications that survive the element check described in Section 2.5, and they are TIC area fractions rather than mass yields. Library assignment can mislead in analytical pyrolysis more generally: a peak can be attributed to the wrong pyrolysis product, and the NIST polymer pyrolysis library defines polyethylene markers only up to C_{23}, partly because chromatographic resolution beyond that is less likely [36].

PET-derived chemistry rose steeply with PET content. Within the campaign that carries the blend series, aromatics and acids went from 0.9 % of the identified area at 10 % PET through 2.4 % at 20 % PET and 11.4 % at 50 % PET to 50.4 % for PET alone, and the number of benzoate-bearing peaks rose from 9 to 74 across the same range. Benzoic acid, which PET pyrolysis releases together with terephthalic acid [37], became a major peak only at 50 % PET and above; at 10 and 20 % PET the same chemistry appeared instead as vinyl benzoate and substituted benzoic acids. Both forms belong to one route. Ester scission is proposed to leave vinyl and carboxyl chain ends, from which benzoic acid forms by decarboxylation or by β-cis-elimination of vinyl benzoate, and substituted benzoic acids such as 4-vinyl- and 4-ethylbenzoic acid are among the quantified primary products of PET [34]. At low PET loading the blends appear to retain more of that route at the vinyl ester stage.

© 2026 The Authors | CC-BY 4.0

Table 3. Py-GCMS at 600 °C, as % of the identified peak area that survives the element check. Aliphatic is olefins, paraffins and cycloalkanes; the misassigned column is the share of total area excluded by that check. The blend series and PET were run in one campaign, HDPE and the 90:10 mixture in an earlier one. Each row is a single run, so no standard deviation is given.

Composition	Campaign	Peaks	Misassigned	Aliphatic	Aromatic + acid	Oxygenated
10 % PET	Mar 2021	330	56.4	84.3	0.9	9.0
20 % PET	Mar 2021	325	55.9	77.0	2.4	13.3
50 % PET	Mar 2021	353	47.7	64.9	11.4	14.5
PET	Mar 2021	193	32.5	3.4	50.4	29.8
HDPE	Oct 2020	310	48.1	79.1	0.0	11.9
90:10 HDPE:PET	Oct 2020	297	55.7	83.6	0.7	5.0

The blends nonetheless stayed aliphatic. Olefins, paraffins and cycloalkanes, the classes into which the diene, 1-alkene and alkane series of polyethylene pyrolysates fall [35], accounted for 84.3 %, 77.0 % and 64.9 % of the identified area at 10, 20 and 50 % PET, against 3.4 % for PET alone. A feed that is half PET by mass still gave a product dominated by polyolefin chain chemistry, which is the product-side counterpart of Section 3.2: the blends follow the polyolefin rather than a weighted average of the two components.

The pure-HDPE and 90:10 runs come from an earlier campaign than the blend series (Table 3). HDPE gave 79.1 % aliphatic area and no detected aromatics, and the 90:10 mixture (the reactor feed of Section 3.4) gave 83.6 %. There is therefore no pure-HDPE reference inside the blend campaign, and the additivity test of Section 3.1.2 has no counterpart here. The composition series also ran at a single temperature, so it carries no kinetic information. Analytical pyrolysis of mixed polymers can also form cross-products that neither polymer gives alone [29], so a blend pyrogram need not be the sum of two independent ones.

3.4 Bench-Scale Pyrolysis

Sections 3.1 and 3.2 work on milligram samples under a controlled ramp. To follow the same feed into the regime a process would use, a 90:10 HDPE:PET charge of approximately 2 g was pyrolysed in a horizontal tube reactor at 450, 500 and 550 °C with a 60 min hold.

3.4.1 Effect of temperature on the product slate

The product is wax, not oil. Wax accounted for 87.6 %, 87.4 % and 83.2 % of the charge at 450, 500 and 550 °C against 4.0–5.1 % recovered as GC-quantifiable liquid (Table 4), a wax-to-liquid ratio between 16 and 22 at every temperature (Fig. 6). A 100 °C rise moved the slate only at its margins: gas nearly tripled, from 0.91 % to 2.42 % of the charge, while wax gave up 4.4 percentage points.

Wax is the primary product of polyethylene pyrolysis when volatiles leave the hot zone quickly. A conical spouted bed gave about 80 % wax from both HDPE and LDPE at 450–600 °C, which the authors attributed to the high gas velocity [38], and in free-fall reactors waxes dominated at low temperature with almost no aromatics, while methane, hydrogen and aromatics rose with temperature and residence time [16]. The tube used here sweeps volatiles out of the furnace and condenses the wax beyond it, and its slate behaves in the same way: wax stayed above 83 % of the charge while gas, methane and BTX rose with temperature. The slate is consistent with a reactor that, under a 60 min hold, depolymerises the feed without cracking the fragments far.

Solid residue was 1.14–1.47 % and fell as temperature rose. This residue and the TGA char are not the same quantity. The reactor residue is the mass left in the vessel from a 2 g charge after 60 min at a set point under argon. The TGA char is what remains of a few milligrams at a measured 550 °C on a ramp under N_2. Charge size, time at temperature and the route by which volatiles escape all differ, so the two can be compared in magnitude only. On that basis, the 13 % char of pure PET in TGA (Section 3.1) corresponds to 1.3 % of a feed carrying 10 % PET, which lies inside the measured range.

Of the hydrocarbons quantified, ethane was the largest at every temperature and grew fastest, from 6.15 mg to 26.35 mg, against 2.46–6.30 mg of methane and 0.14–0.32 mg of hydrogen (Table 5). Methane and hydrogen rose with temperature, as they do in polyethylene pyrolysis, where ethylene, the direct product of β-scission, is generally the main gas [16]. Ethylene and the C_3–C_4 hydrocarbons were not calibrated here, and ethane was quantified on the methane response factor, so these figures describe part of the gas rather than its composition.

CO_2 appeared at all three temperatures, at 8.44, 15.91 and 14.61 mg, and is the one product that can only come from the ester groups of PET [18, 27]. It corresponds to 4.5–7.9 % of the PET charged, or 1.9–3.5 % of its carbon, against up to 21 % CO_2 from PET alone micropyrolysed at 600 °C [34]. Less than a fifth of the carbon in the PET carbonyl groups therefore left as CO_2. Carbon monoxide, the other decarbonylation route, was not calibrated, and benzoic acid, vinyl benzoate, terephthalate esters and benzene are the main condensable products of PET [30]. The remainder is therefore likely held in CO, in the residue and in oxygenated condensables that the retention-time classes of Table 4 do not separate.

In the liquid, BTX rose from 0.153 % to 0.242 % of the charge between 450 and 550 °C, a 58 % relative increase on a fraction that stays below 0.25 % throughout. Two sources can supply it: benzene is among the major condensable products of PET [30], and aromatics also form from polyethylene wax through secondary reactions [39]. The present data do not separate the two. The C_6–C_{12} aliphatics, which carry 86–93 % of the quantified liquid, moved from 4.01 % to 3.71 % to 4.74 % without a monotonic trend. The aromatics that the PET fraction supplies do not accumulate in the condensate.

The balance closed to 94.6 %, 94.7 % and 91.9 % of the charge: level between 450 and 500 °C, then 2.8 percentage points lower at 550 °C. The gas analysis quantified CH_4, C_2H_6, CO_2 and H_2 only, leaving ethylene, the C_3–C_4 hydrocarbons and CO outside the accounting. The unaccounted 5–8 % therefore includes these gases, together with any wax or liquid lost on recovery. The uncalibrated gases are the ones expected to grow with temperature, so the larger shortfall at 550 °C may reflect underestimated gas and gives no measure of the extent of cracking.

3.4.2 Effect of feed ratio

Feed composition moves the product yields of a mixed-plastic pyrolysis [10]. One run on an 80:20 feed at 550 °C gives an indication of that effect here, within two limits. The run was held for 120 min against 60 min for 90:10, and its liquid was not worked up against the internal standard, so it is described by fractions of the quantified chromatogram area and not by yields. Of that area, BTX was 8.2 % for the 80:20 feed against 5.9 % for 90:10, the fraction eluting after *n*-C_{12} 15.9 % against 3.0 %, and C_6–C_{12} 75.9 % against 91.1 %. The liquid from the PET-richer feed thus carried more aromatics and more heavy ends. Because hold time changed together with feed ratio, the difference cannot be assigned to PET content alone.

3.5 Implications for Mixed-Feed Pyrolysis

The PET loadings tested here are within the range found in real waste. PET makes up on average 7.6 % of polymer waste in Europe [30], and PET bottles made up 33.2 % and 61.4 % of seashore and underwater litter collected for pyrolysis, enough that PET had to be sorted out first [40].

The window in which additivity fails is the window in which the reactor runs. Blends lost 19–41 % more of their initial mass than Eq. (1) predicts between 400 °C and 500 °C, and at 450 °C, the lowest bench-scale set point, the reactor had already carried 93.1 % of a 2 g charge into wax, liquid and gas. The mass-weighted superposition of the pure-polymer curves thus under-predicts mass loss at the design point, not in some tail of the operating range. No kinetic model was fitted in this work. A scheme that treats HDPE and PET as decomposing independently reduces to the same superposition, and would be expected to carry the same bias.

© 2026 The Authors | CC-BY 4.0

Table 4. Product distribution and liquid speciation for the 90:10 HDPE:PET feed, as % of the charge. Liquid is the sum of the three right-hand columns, quantified by GC-FID against an adamantane internal standard; wax and residue were weighed. Hold time 60 min. One run per temperature.

	Product distribution					Liquid speciation		
T (°C)	Wax	Liquid	Gas	Residue	Total	BTX	C_6–C_{12}	C_{12}^+
450	87.59	4.64	0.91	1.47	94.61	0.153	4.01	0.479
500	87.39	3.98	1.98	1.32	94.67	0.160	3.71	0.118
550	83.20	5.14	2.42	1.14	91.90	0.242	4.74	0.157

Table 5. Permanent gas from the 90:10 HDPE:PET feed, in mg, quantified against an argon internal standard; C_2H_6 on the CH_4 response factor. C_2H_4, C_3–C_4 hydrocarbons and CO were not calibrated. One run per temperature.

T (°C)	CH_4	C_2H_6	CO_2	H_2	Total
450	2.46	6.15	8.44	0.14	17.19
500	4.62	18.93	15.91	0.17	39.63
550	6.30	26.35	14.61	0.32	47.58

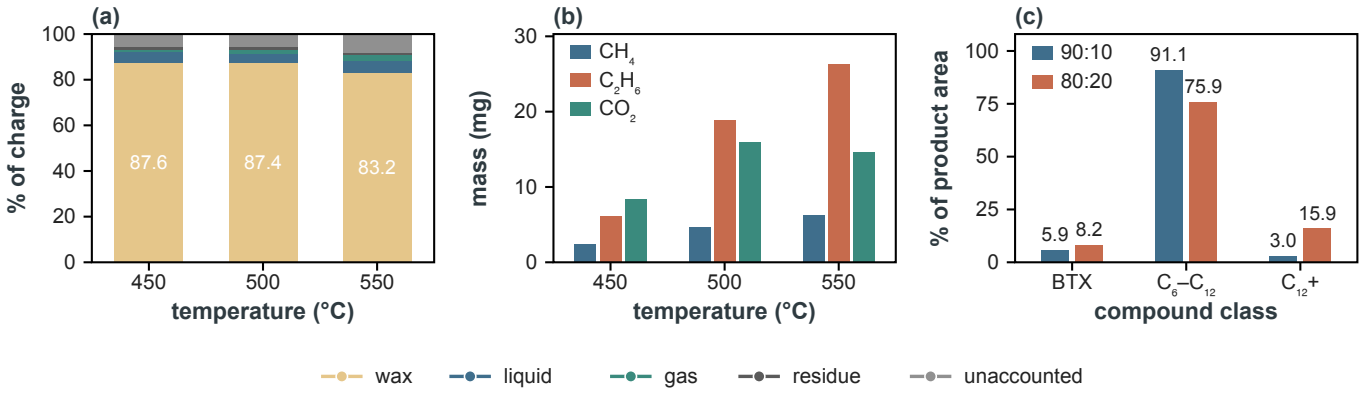


Figure 6. Bench-scale products. (a) product distribution for the 90:10 feed as % of the charge, grey being the balance shortfall; the label gives the wax share. (b) permanent gas by species; H_2 ($\leq$0.32 mg) is left to Table 5. (c) liquid composition at 550 °C by feed ratio, as % of quantified product area rather than yields; the 80:20 run was held 120 min against 60 min.

The deviation had one sign. Interactions in mixed-plastic pyrolysis have been reported in both directions [25, 26]; here all six blend–campaign combinations deviated in the same direction. Between 10 and 50 % PET, the range tested, a mixed charge lost mass earlier than the sum of its parts, so the bias would not average out over feed compositions within that range. The deviation did not increase in proportion to PET content in either campaign, but the ranking of the blends was not reproduced (Section 3.1.2), and the form of a composition correction remains open.

What the bench-scale runs add is the product slate of a PET-bearing feed. Under a 60 min hold the slate stayed wax-dominant at 83–88 % across 450–550 °C, and BTX stayed below 0.25 % of the charge. The reactor runs had no pure-HDPE comparator, so this slate cannot be attributed to PET: polyethylene alone gives a wax-dominant product in reactors that remove volatiles quickly [38]. Read together with the earlier onset of the aliphatic channel (Section 3.2), one interpretation is that the interaction advances the onset of decomposition without advancing cracking. The reactor data are compatible with that interpretation and do not test it. If it holds, a process targeting fuel-range liquid would gain more from residence time and secondary cracking than from a higher primary pyrolysis temperature.

A wax-dominant slate is not in itself a loss: polyolefin pyrolysis waxes are among the feeds proposed for co-processing in existing refinery units [41]. What PET adds is oxygen. Most of its carbonyl carbon did not leave as CO_2 (Section 3.4), PET and PVC in a pyrolysis feed yield corrosive gases and sublimating substances that lower product quality and damage the treatment plant [42], and post-consumer pyrolysis oils already carry more than ten times the oxygen a steam cracker accepts [12]. Where the rest of the PET oxygen goes (into CO, the residue or the wax) was not measured here. It is needed, alongside the conversion rate, to judge whether a PET-bearing polyolefin stream can be pyrolysed without first sorting PET out.

The study has limits that bound these statements. Every thermogravimetric, Py-GCMS and reactor measurement is a single run, and only HDPE and the 90:10 mixture were repeated in EGA-MS, so no result carries a standard deviation and the reproducibility of the additivity test rests on its repetition in a second campaign. Three blend compositions and two temperature programmes were tested, which establishes the sign and scale of the deviation but neither its dependence on PET content nor its dependence on heating rate. The reactor series had no pure-HDPE run, and its gas analysis left ethylene, the C_3–C_4 hydrocarbons and CO unquantified. The mechanism of the interaction was not tested.

4. CONCLUSIONS

We compared the thermal decomposition of HDPE–PET blends containing 10, 20 and 50 % PET with the mass-weighted sum of the pure polymers by TGA, EGA-MS and Py-GCMS, and followed a 90:10 feed into a bench-scale tube reactor. Every blend lost more mass than additivity predicts, with maximum deviations of 19–41 % of the initial mass at 400–500 °C in two campaigns run at 9.8 and 20.3 °C min^{-1}. The sign and scale of the deviation were reproduced between the campaigns, and the ranking of the blends was not. The volatile maximum of every blend stayed within 5 °C of HDPE, while the aliphatic channel of the blends left the baseline 14–24 °C earlier than that of HDPE, against a repeatability of 2 °C. The earlier mass loss therefore includes an earlier onset of the polyolefin fraction, at an unchanged temperature of maximum release. In the reactor, wax made up 83–88 % of the charge across 450–550 °C, a slate that cannot be assigned to PET without a pure-HDPE run. The earlier onset is consistent with initiation by PET-derived species or with a phys-

© 2026 The Authors | CC-BY 4.0

ical effect of the shared melt, and neither was tested. For PET-bearing polyolefin feeds, the additive superposition of pure-polymer curves underestimates mass loss in the window where a pyrolysis reactor operates. Replicated runs over more compositions, a pure-HDPE reactor comparator and isotopic labelling would establish the composition dependence, the effect at gram scale and the mechanism.

CRediT AUTHORSHIP CONTRIBUTION STATEMENT

Aulia Annas Mufti: Formal analysis, Visualization, Writing – original draft, Writing – review & editing. **Neza Rahayu Palapa:** Formal analysis, Validation, Writing – review & editing. **Muhamad F. Arif:** Validation, Writing – review & editing. **Tarmizi Taher:** Conceptualization, Methodology, Investigation, Data curation, Formal analysis, Writing – original draft, Supervision, Project administration.

DECLARATION OF COMPETING INTEREST

The authors declare that they have no known competing financial interests or personal relationships that could have appeared to influence the work reported in this paper.

DATA AVAILABILITY

Data will be made available on request.

FUNDING

This research received no external funding.

ACKNOWLEDGEMENTS

The authors thank the Institute of Regional Innovation (IRI), Hirosaki University, for providing the research facilities used in this work.

REFERENCES

[1] R. Geyer, J. R. Jambeck, K. L. Law, Production, use, and fate of all plastics ever made, Science Advances 3 (2017) e1700782. doi:10.1126/sciadv.1700782.

[2] J. R. Jambeck, R. Geyer, C. Wilcox, T. R. Siegler, M. Perryman, A. Andrady, R. Narayan, K. L. Law, Plastic waste inputs from land into the ocean, Science 347 (2015) 768–771. doi:10.1126/science.1260352.

[3] W. W. Y. Lau, Y. Shiran, R. M. Bailey, E. Cook, M. R. Stuchtey, J. Koskella, C. A. Velis, L. Godfrey, J. Boucher, M. B. Murphy, R. C. Thompson, E. Jankowska, A. Castillo Castillo, T. D. Pilditch, B. Dixon, L. Koerselman, E. Kosior, E. Favoino, J. Gutberlet, S. Baulch, M. E. Atreya, D. Fischer, K. K. He, M. M. Petit, U. R. Sumaila, E. Neil, M. V. Bernhofen, K. Lawrence, J. E. Palardy, Evaluating scenarios toward zero plastic pollution, Science 369 (2020) 1455–1461. doi:10.1126/science.aba9475.

[4] K. Ragaert, L. Delva, K. Van Geem, Mechanical and chemical recycling of solid plastic waste, Waste Management 69 (2017) 24–58. doi:10.1016/j.wasman.2017.07.044.

[5] M. Roosen, N. Mys, M. Kusenberg, P. Billen, A. Dumoulin, J. Dewulf, K. M. Van Geem, K. Ragaert, S. De Meester, Detailed analysis of the composition of selected plastic packaging waste products and its implications for mechanical and thermochemical recycling, Environmental Science & Technology 54 (2020) 13282–13293. doi:10.1021/acs.est.0c03371.

[6] I. Antonopoulos, G. Faraca, D. Tonini, Recycling of post-consumer plastic packaging waste in the EU: Recovery rates, material flows, and barriers, Waste Management 126 (2021) 694–705. doi:10.1016/j.wasman.2021.04.002.

[7] S. Al-Salem, A. Antelava, A. Constantinou, G. Manos, A. Dutta, A review on thermal and catalytic pyrolysis of plastic solid waste (PSW), Journal of Environmental Management 197 (2017) 177–198. doi:10.1016/j.jenvman.2017.03.084.

[8] I. Vollmer, M. J. F. Jenks, M. C. P. Roelands, R. J. White, T. van Harmelen, P. de Wild, G. P. van der Laan, F. Meirer, J. T. F. Keurentjes, B. M. Weckhuysen, Beyond mechanical recycling: Giving new life to plastic waste, Angewandte Chemie International Edition 59 (2020) 15402–15423. doi:10.1002/anie.201915651.

[9] O. Dogu, M. Pelucchi, R. Van de Vijver, P. H. Van Steenberge, D. R. D'hooge, A. Cuoci, M. Mehl, A. Frassoldati, T. Faravelli, K. M. Van Geem, The chemistry of chemical recycling of solid plastic waste via pyrolysis and gasification: State-of-the-art, challenges, and future directions, Progress in Energy and Combustion Science 84 (2021) 100901. doi:10.1016/j.pecs.2020.100901.

[10] H. C. Genuino, M. Pilar Ruiz, H. J. Heeres, S. R. Kersten, Pyrolysis of mixed plastic waste: Predicting the product yields, Waste Management 156 (2023) 208–215. doi:10.1016/j.wasman.2022.11.040.

[11] H. C. Genuino, M. C. P. van Eijk, S. R. A. Kersten, M. P. Ruiz, Pyrolysis of real packaging plastic waste streams in a fluidized-bed pilot plant, Energy & Fuels 38 (2024) 2188–2199. doi:10.1021/acs.energyfuels.3c04114.

[12] M. Kusenberg, A. Eschenbacher, M. R. Djokic, A. Zayoud, K. Ragaert, S. De Meester, K. M. Van Geem, Opportunities and challenges for the application of post-consumer plastic waste pyrolysis oils as steam cracker feedstocks: To decontaminate or not to decontaminate?, Waste Management 138 (2022) 83–115. doi:10.1016/j.wasman.2021.11.009.

[13] G. Grause, S. Matsumoto, T. Kameda, T. Yoshioka, Pyrolysis of mixed plastics in a fluidized bed of hard burnt lime, Industrial & Engineering Chemistry Research 50 (2011) 5459–5466. doi:10.1021/ie102412h.

[14] R. Prurapark, K. Owjaraen, B. Saengphrom, I. Limthongtip, N. Tongam, Effect of temperature on pyrolysis oil using high-density polyethylene and polyethylene terephthalate sources from mobile pyrolysis plant, Frontiers in Energy Research 8 (2020) 541535. doi:10.3389/fenrg.2020.541535.

[15] M. Konarova, N. Batalha, G. Fraga, M. H. Ahmed, S. Pratt, B. Laycock, Integrating PET chemical recycling with pyrolysis of mixed plastic waste via pressureless alkaline depolymerization in a hydrocarbon solvent, Waste Management 174 (2024) 24–30. doi:10.1016/j.wasman.2023.11.023.

[16] J. F. Mastral, C. Berrueco, J. Ceamanos, Pyrolysis of high-density polyethylene in free-fall reactors in series, Energy & Fuels 20 (2006) 1365–1371. doi:10.1021/ef060007n.

[17] M. K. M. Handawy, T. M. Abdellatief, X. Duan, T. Salameh, A.-K. Hamid, M. Hussein, Kinetic insights into high-density polyethylene, polyethylene terephthalate, and their blend using thermogravimetric analysis and model-free methods, Fuel Processing Technology 282 (2026) 108390. doi:10.1016/j.fuproc.2025.108390.

[18] A. Dhahak, G. Hild, M. Rouaud, G. Mauviel, V. Burkle-Vitzthum, Slow pyrolysis of polyethylene terephthalate: Online monitoring of gas production and quantitative analysis of waxy products, Journal of Analytical and Applied Pyrolysis 142 (2019) 104664. doi:10.1016/j.jaap.2019.104664.

[19] P. Das, P. Tiwari, Thermal degradation study of waste polyethylene terephthalate (PET) under inert and oxidative environments, Thermochimica Acta 679 (2019) 178340. doi:10.1016/j.tca.2019.178340.

[20] A. Aboulkas, K. El harfi, A. El Bouadili, Thermal degradation behaviors of polyethylene and polypropylene. part i: Pyrolysis kinetics and mechanisms, Energy Conversion and Management 51 (7) (2010) 1363–1369. doi:10.1016/j.enconman.2009.12.017.

[21] Z. Alhulaybi, I. Dubdub, Comprehensive kinetic study of PET pyrolysis using TGA, Polymers 15 (14) (2023) 3010. doi:10.3390/polym15143010.

[22] N. Netsch, L. Schröder, M. Zeller, I. Neugber, D. Merz, C. O. Klein, S. Tavakkol, D. Stapf, Thermogravimetric study on thermal degradation kinetics and polymer interactions in mixed thermoplastics, Journal of Thermal Analysis and Calorimetry 150 (2024) 211–229. doi:10.1007/s10973-024-13630-6.

[23] G. Martínez-Narro, N. J. Royston, K. L. Billsborough, A. N. Phan, Kinetic modelling of mixed plastic waste pyrolysis, Chemical Thermodynamics and Thermal Analysis 9 (2023) 100105. doi:10.1016/j.ctta.2023.100105.

[24] A. Snegirev, M. K. Handawy, V. Stepanov, V. Talalov, Pyrolysis and combustion of polymer mixtures: Exploring additivity of the heat release rate, Polymer Degradation and Stability 161 (2019) 245–259. doi:10.1016/j.polymdegradstab.2019.01.037.

[25] J. Briceno, M. A. Lemos, F. Lemos, Kinetic analysis of the degradation of HDPE + PP polymer mixtures, International Journal of Chemical Kinetics 53 (2021) 660–674. doi:10.1002/kin.21472.

[26] I. Dubdub, M. Al-Yaari, Pyrolysis of mixed plastic waste: I. kinetic study, Materials 13 (21) (2020) 4912. doi:10.3390/ma13214912.

[27] P. T. Williams, E. A. Williams, Interaction of plastics in mixed-plastics pyrolysis, Energy & Fuels 13 (1) (1998) 188–196. doi:10.1021/ef980163x.

[28] N. V. Muravyev, S. Vyazovkin, The status of pyrolysis kinetics studies by thermal analysis: Quality is not as good as it should and can readily be, Thermo 2 (2022) 435–452. doi:10.3390/thermo2040029.

[29] I. Coralli, V. Giorgi, I. Vassura, A. G. Rombolà, D. Fabbri, Secondary reactions in the analysis of microplastics by analytical pyrolysis, Journal of Analytical and Applied Pyrolysis 161 (2022) 105377. doi:10.1016/j.jaap.2021.105377.

[30] A. Brems, J. Baeyens, C. Vandecasteele, R. Dewil, Polymeric cracking of waste polyethylene terephthalate to chemicals and energy, Journal of the Air & Waste Management Association 61 (2011) 721–731. doi:10.3155/1047-3289.61.7.721.

[31] F. Richter, G. Rein, The role of heat transfer limitations in polymer pyrolysis at the microscale, Frontiers in Mechanical Engineering 4 (2018) 18. doi:10.3389/fmech.2018.00018.

[32] R. Tuffi, S. D'Abramo, L. M. Cafiero, E. Trinca, S. Vecchio Ciprioti, Thermal

© 2026 The Authors | CC-BY 4.0

behavior and pyrolytic degradation kinetics of polymeric mixtures from waste packaging plastics, Express Polymer Letters 12 (2018) 82–99. doi:10.3144/expresspolymlett.2018.7.

[33] R. Singh, B. Ruj, A. Sadhukhan, P. Gupta, A TG-FTIR investigation on the co-pyrolysis of the waste HDPE, PP, PS and PET under high heating conditions, Journal of the Energy Institute 93 (2020) 1020–1035. doi:10.1016/j.joei.2019.09.003.

[34] B. A. Perez, H. E. Toraman, Intrinsic kinetics of polyethylene terephthalate pyrolysis via micropyrolysis and multivariate chromatographic analysis, ACS Engineering Au 6 (2025) 90–104. doi:10.1021/acsengineeringau.5c00055.

[35] G. Biale, J. La Nasa, M. Mattonai, A. Corti, V. Vinciguerra, V. Castelvetro, F. Modugno, A systematic study on the degradation products generated from artificially aged microplastics, Polymers 13 (2021) 1997. doi:10.3390/polym13121997.

[36] E. P. Erisman, Y. Simón-Manso, W. E. Wallace, NIST polymer pyrolysis search: A new pyrolysis GC–MS search program and mass spectral reference library, Environmental Science & Technology 60 (2026) 19336–19346. doi:10.1021/acs.est.5c18872.

[37] T. Yoshioka, G. Grause, C. Eger, W. Kaminsky, A. Okuwaki, Pyrolysis of poly(ethylene terephthalate) in a fluidised bed plant, Polymer Degradation and Stability 86 (3) (2004) 499–504. doi:10.1016/j.polymdegradstab.2004.06.001.

[38] R. Aguado, M. Olazar, M. J. San José, B. Gaisán, J. Bilbao, Wax formation in the pyrolysis of polyolefins in a conical spouted bed reactor, Energy & Fuels 16 (2002) 1429–1437. doi:10.1021/ef020043w.

[39] G. Elordi, G. Lopez, M. Olazar, R. Aguado, J. Bilbao, Product distribution modelling in the thermal pyrolysis of high density polyethylene, Journal of Hazardous Materials 144 (2007) 708–714. doi:10.1016/j.jhazmat.2007.01.101.

[40] A. Veksha, A. Ahamed, X. Y. Wu, L. Liang, W. P. Chan, A. Giannis, G. Lisak, Technical and environmental assessment of laboratory scale approach for sustainable management of marine plastic litter, Journal of Hazardous Materials 421 (2022) 126717. doi:10.1016/j.jhazmat.2021.126717.

[41] R. Palos, A. Gutiérrez, F. J. Vela, M. Olazar, J. M. Arandes, J. Bilbao, Waste refinery: The valorization of waste plastics and end-of-life tires in refinery units. a review, Energy & Fuels 35 (2021) 3529–3557. doi:10.1021/acs.energyfuels.0c03918.

[42] S. Kumagai, T. Yoshioka, Feedstock recycling via waste plastic pyrolysis, Journal of the Japan Petroleum Institute 59 (2016) 243–253. doi:10.1627/jpi.59.243.

© 2026 The Authors | CC-BY 4.0